

Received April 15, 2019, accepted May 7, 2019, date of publication May 14, 2019, date of current version June 6, 2019.

Digital Object Identifier 10.1109/ACCESS.2019.2916655

# A Compact Planar Quasi-Yagi Antenna With Bandpass Filtering Response

GUI LIU, YONG MEI PAN<sup>1</sup>, (Senior Member, IEEE), TIAN LI WU,  
AND PENG FEI HU<sup>1</sup>, (Student Member, IEEE)

School of Electronic and Information Engineering, South China University of Technology, Guangzhou 510641, China

Corresponding author: Yong Mei Pan (eeympa@scut.edu.cn)

This work was supported in part by the National Natural Science Foundation of China under Grant 61871187, and in part by the Guangdong Natural Science Funds for Distinguished Young Scholars under Grant 2016A030306007.

**ABSTRACT** A planar quasi-Yagi antenna with bandpass filtering response is presented. The quasi-Yagi antenna consists of a double-sided printed driven dipole, an offset double-sided parallel-strip line (DSPSL) director, a DSPSL reflector, and an offset DSPSL parasitic element. Both the reflector and the parasitic element can produce an extra radiation null at the band-edges of the passband, and the parasitic element can also generate an additional resonance within the passband. As a result, a compact wideband quasi-Yagi antenna with quasi-elliptic bandpass filtering response is obtained, without requiring any extra filtering circuit. In addition, the antenna is fed by a balanced DSPSL, and therefore, no balun is needed, leading to a very simple feeding structure. For demonstration, a prototype operating at 2.4 GHz was designed and measured. The prototype has a low profile of  $0.006\lambda_0$ , a  $-10$ -dB impedance bandwidth of 30.4%, an average gain of 5.7 dBi over the passband, and an out-of-band suppression level of about 20 dB in the near stopbands.

**INDEX TERMS** Filtering antenna, quasi-Yagi antenna, DSPSL.

## I. INTRODUCTION

With the rapid development of modern wireless communication system, it is highly demanded to develop new devices or components that feature low cost, miniaturized size, multiple functions, etc. The filtering antenna, which integrates the functions of the antenna and the filter, has therefore attracted increasing attention due to its enhanced integration level [1]–[9]. Generally, the integration was realized by inserting a specifically designed bandpass filter into the feeding network of antenna [1]–[5]. Good filtering performance could be obtained but the antenna performance would be degraded to a certain extent owing to the inevitable insertion loss of the filtering circuits. To address this issue, it was proposed using simple parasitic elements such as shorting pins, slot, or microstrip-stub instead of the complex bandpass filter to control the input impedance of antenna, and hence realize the filter-like frequency response [6]–[9]. In this way, both good filtering and efficient radiating performances can be simultaneously achieved, without increasing either the footprint or the loss of the antenna.

Quasi-Yagi antenna, which evolved from the classical Yagi-Uda antenna is of planar structure, and thus is easy

to be fabricated and also easy to be integrated with other circuits [10]–[15]. Studies of quasi-Yagi antenna mainly concentrated on developing various antenna geometries [10], excitation schemes [11], and bandwidth [14] or gain [15] enhancement techniques. Recently, the research interest has also been extended to the quasi-Yagi antenna with filtering response [16]–[21]. Various design schemes were developed, but most of them needed to use specific filtering circuits such as the balanced-to-unbalanced bandpass filter [16], the load-insensitive multilayer balun filter [17], the double-sided parallel-strip line (DSPSL) filter [18], or the bandstop filter [20], for the implementation of filtering function, which introduced additional insertion loss and degraded antenna efficiency undesirably, as discussed above. To the best of our knowledge, there is only one filtering quasi-Yagi antenna achieving filtering response without involving extra filtering circuit [21]. Instead, just a parasitic loop was used to enhance the selectivity of the upper band-edge. However, the resultant filtering performance is not very satisfactory, and the suppression level in the stop-band is only about 10 dB. In addition, to provide a balanced current for the driven dipole, an additional coaxial balun was required on the feeding cable.

The DSPSL [22]–[24], as a kind of balanced transmission line, had been used in the design of quasi-Yagi antenna to

The associate editor coordinating the review of this manuscript and approving it for publication was Choon Ki Ahn.

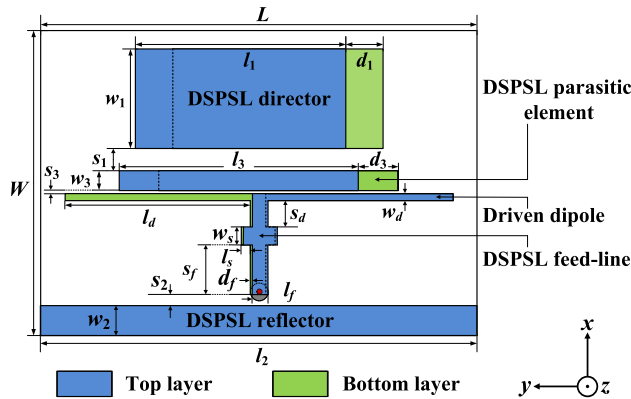


FIGURE 1. Configuration of the proposed filtering quasi-Yagi antenna.

TABLE 1. Dimensions of the proposed filtering antenna.

Parameters	$L$	$W$	$l_d$	$w_d$	$s_d$	$l_1$
Value/mm	70	49	29.8	1.3	4.1	34
Parameters	$w_1$	$d_1$	$s_1$	$l_2$	$w_2$	$s_2$
Value/mm	16.1	6.1	3.56	70	5	1.5
Parameters	$l_3$	$w_3$	$d_3$	$s_3$	$l_s$	$w_s$
Value/mm	38.85	3.4	6.4	0.34	1.55	3
Parameters	$l_f$	$s_f$	$d_f$			
Value/mm	2.6	8	0.4			

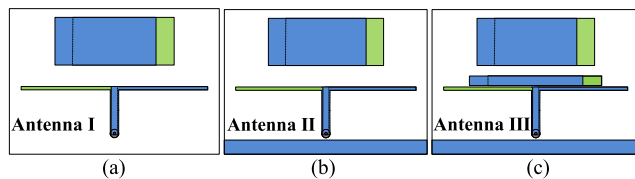


FIGURE 2. Configurations of the reference antennas. (a) Antenna I composed of a driven dipole and a director. (b) Antenna II composed of a driven dipole, a director, and also a reflector. (c) Antenna III having an extra parasitic element.

eliminate the extra balun [24]. Broad bandwidth of 73.3% was obtained, but exhibiting no filtering response. In this paper, slight modifications are introduced in the DSPSL-based quasi-Yagi antenna [24] to integrate the filtering function. Specifically, two radiation nulls are introduced at the edges of the passband with the aid of the reflector and a DSPSL parasitic element, enhancing the out-of-band suppression level to about 20 dB. A quasi-elliptic bandpass filtering response is thus achieved without using any extra filtering circuit. The operating principle is analyzed in detail, and a prototype was fabricated and measured to verify the design concept.

## II. ANTENNA DESIGN

### A. ANTENNA CONFIGURATION

The configuration of the proposed filtering quasi-Yagi antenna is depicted in Fig. 1. It consists of a driven dipole (length  $l_d$ , width  $w_d$ ), an offset DSPSL director (length  $l_1$ , width  $w_1$ , offset distance  $d_1$ ), a DSPSL reflector (length  $l_2$ , width  $w_2$ ), and an offset DSPSL parasitic element (length  $l_3$ , width  $w_3$ , offset distance  $d_3$ ). The driven dipole is fed by an

offset DSPSL (offset distance  $d_f$ ) with short stubs. Here, it should be mentioned that the reason why the offset DSPSL structure is utilized in the antenna is because it can provide higher degree of design freedom compared to the non-offset counterpart, and thus lead to a superior performance. As shown in Fig. 1, the entire filtering quasi-Yagi antenna is double-sided printed on the top and bottom layers of a single substrate with a dielectric constant of  $\epsilon_r = 2.94$  and a thickness of  $h = 0.8$  mm. The detailed dimensions are listed in Table 1.

As the director, the reflector, the parasitic element, along with the feeding line of the proposed quasi-Yagi antenna are all based on the DSPSL structure, the resonance frequency and the characteristic impedance of each part can be estimated roughly via the formulae given in [24]. In particular, when using the parameters of Table 1, the resonance frequency is calculated to be 2.50 GHz for the director, and 2.40 GHz for the parasitic element. Meanwhile, the calculated characteristic impedance of the feeding DSPSL ( $56.1 \Omega$ ) is found very close to  $50 \Omega$ , which can match well to a simple coaxial cable without needing extra transformer. For the driven dipole, the resonance frequency is about 2 GHz.

### B. ANTENNA MECHANISM

In this subsection, three reference antennas are investigated together with the proposed filtering quasi-Yagi antenna to show its operating mechanism. As shown in Fig. 2, Antenna I is a quasi-Yagi antenna just having a driven dipole and a director, Antenna II is a quasi-Yagi antenna having a driven dipole, a director and also a reflector, whereas Antenna III is a quasi-Yagi antenna having an extra DSPSL parasitic element. To facilitate the comparison, all the dimensions of the three reference antennas are chosen the same as that of the proposed design. Fig. 3 shows the simulated reflection coefficients and realized gains in the end-fire direction ( $+x$  axis), as a function of frequency. With reference to the green dot dash line, only one resonant mode is excited at 2.02 GHz in the passband of Antenna I. By looking into the current distribution on the antenna, this mode is identified as the fundamental mode of the driven dipole. It is notable that the feeding DSPSL also generates a resonance at 2.54 GHz, but the resonance is too weak to radiate effectively. Both the input impedance and end-fire gain vary gradually with the frequency and exhibit no obvious filtering response. When a DSPSL reflector is introduced in Antenna II, the original weak resonance at 2.54 GHz slightly shifts to 2.30 GHz due to the loading effect of the reflector. In addition, it is interesting to note that a radiation minimum is achieved at 1.65 GHz. This radiation minimum improves the roll-off rate at the lower band-edge greatly, and hence realizes filtering response in the lower band. Next, to enhance the selectivity of the upper band, an offset DSPSL parasitic element is used in Antenna III. It can be seen from the red dot line that owing to the parasitic element, a new resonance is generated at 2.62 GHz, and simultaneously, the impedance matching has a significant improvement over the entire operating band. This is due to

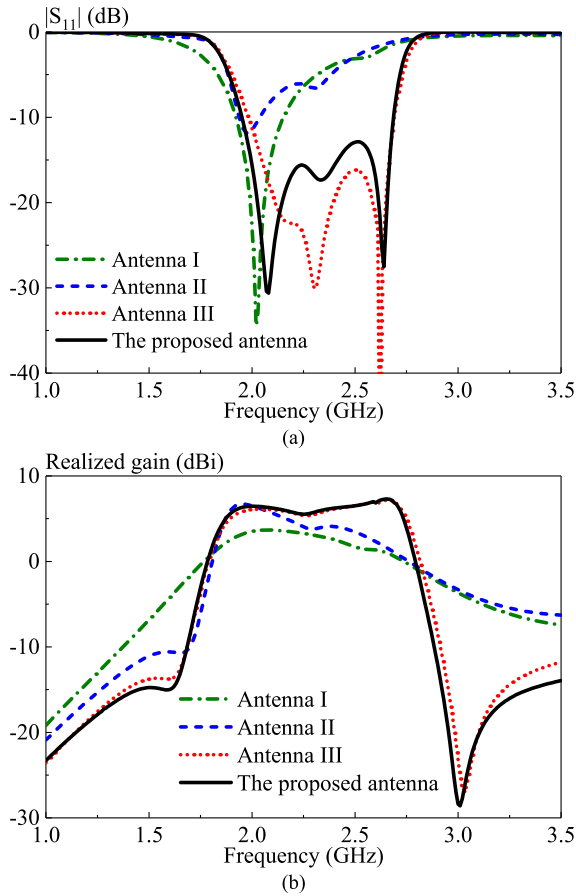


**FIGURE 3.** Simulated reflection coefficients and end-fire gains of the reference and the proposed antennas. (a) Reflection coefficients. (b) End-fire gains.

the fact that the coupling between the driven dipole and the director is enhanced via the parasitic element which is located in-between. The three resonant modes with adjacent resonance frequencies form a wide impedance passband, which features a  $-10$ -dB bandwidth of 30.4% (1.98-2.69 GHz) and a nearly flat gain of about 6.2 dBi. On the other hand, a new

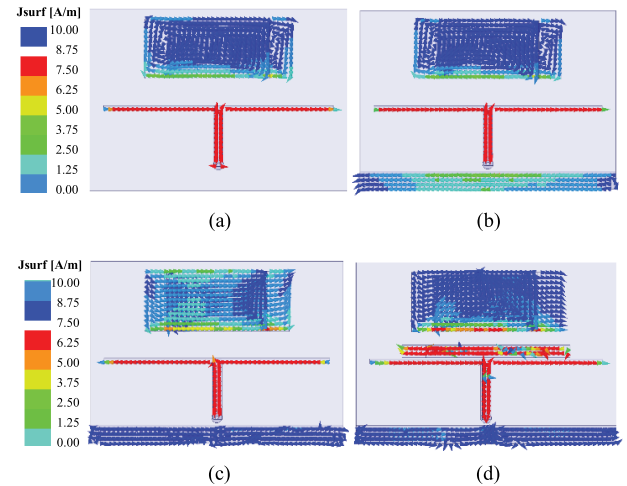


**FIGURE 4.** Surface current distributions on reference Antennas I, II, and III. (a) Antenna I at 1.65 GHz. (b) Antenna II at 1.65 GHz. (c) Antenna II at 3.03 GHz. (d) Antenna III at 3.03 GHz.

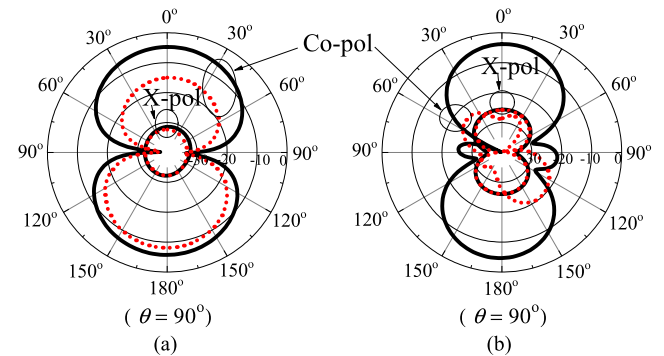


**FIGURE 5.** Radiation patterns of the reference Antenna I and the proposed antenna in the  $xy$ -plane ( $E$ -plane). (a) 1.58 GHz. (b) 3.01 GHz. — Antenna I ..... The proposed antenna.

radiation null is achieved at 3.03 GHz, as shown in Fig. 3(b). This null substantially improves the filtering performance in the upper stop-band, and consequently leads to a quasi-elliptic band-pass filtering response. Finally, in the proposed antenna, a pair of very short stubs is introduced in the feeding

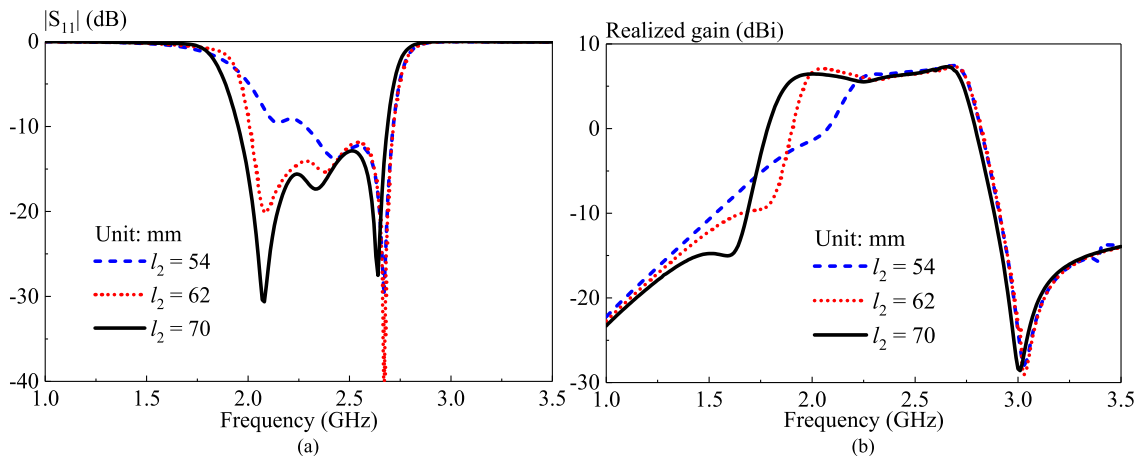


**FIGURE 6.** Simulated reflection coefficients and end-fire gains of the proposed antenna for different lengths  $l_2$  of the reflector. (a) Reflection coefficients for different  $l_2$ . (b) End-fire gains for different  $l_2$ .

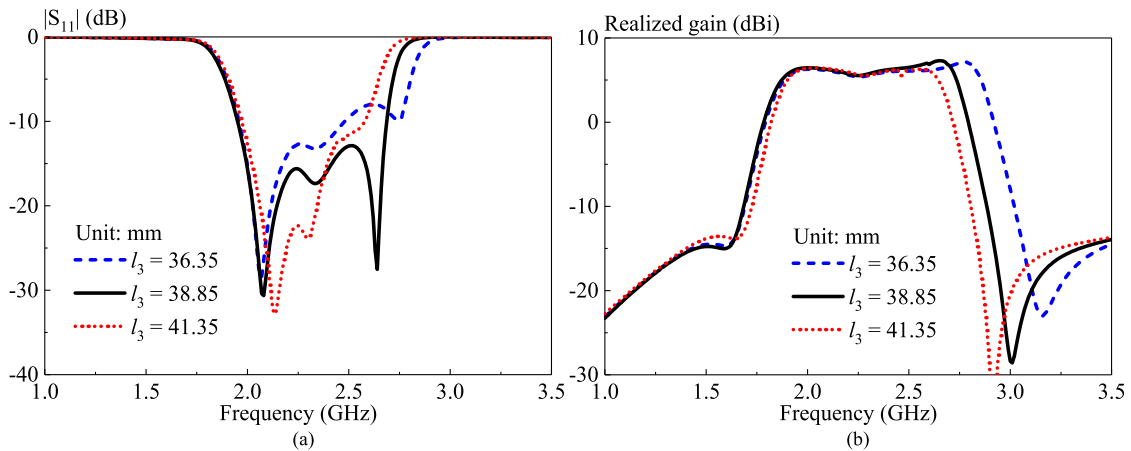


**FIGURE 7.** Simulated reflection coefficients and end-fire gains of the proposed antenna for different lengths  $l_3$  of the parasitic element. (a) Reflection coefficients for different  $l_3$ . (b) End-fire gains for different  $l_3$ .

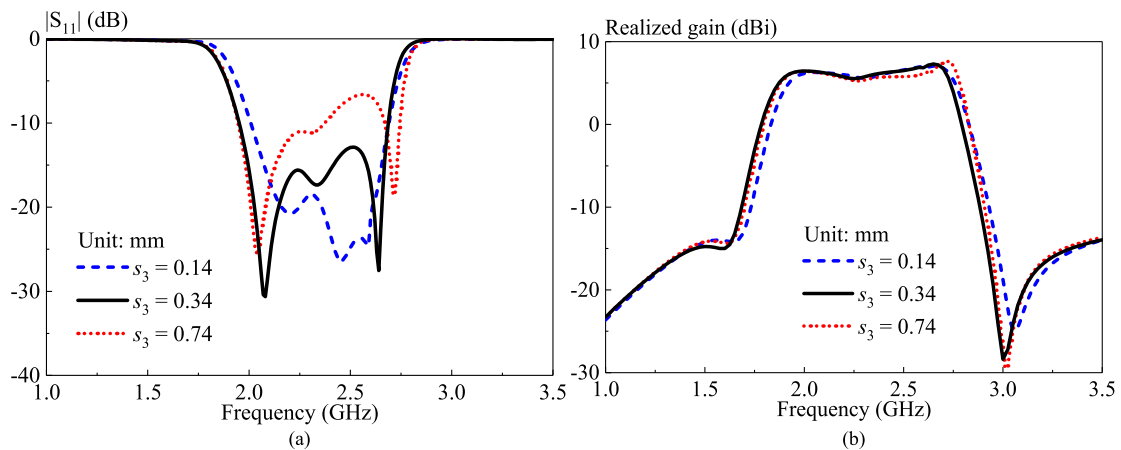


**FIGURE 8.** Simulated reflection coefficients and end-fire gains of the proposed antenna for different spacing  $s_3$  between the dipole and parasitic element. (a) Reflection coefficients for different  $s_3$ . (b) End-fire gains for different  $s_3$ .

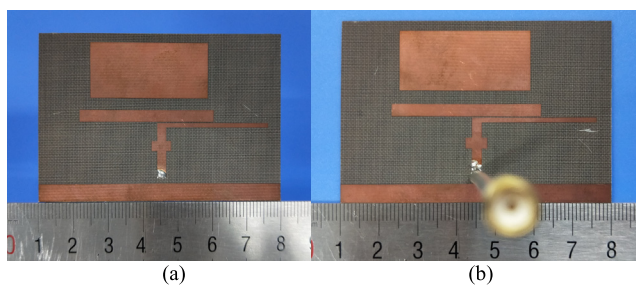


**FIGURE 9.** Photographs showing the prototype of the proposed filtering antenna. (a) The photo showing the top view. (b) The photo showing the bottom view.

DSPSL (Fig. 1). It can be seen that the performance of the proposed antenna is very close to that of Antenna III, except that the suppression level is further improved to over 20 dB in both the lower and upper stopbands.

### C. ANALYSIS OF RADIATION NULLS

As shown above, the introduction of the reflector and the parasitic element brings about a radiation null on each side of the passband, which plays an important role in obtaining

the filtering function. Therefore, it is of significance to further investigate the generative mechanism of the two radiation nulls. Fig. 4 compares the simulated surface current distributions of Antennas I (Fig. 4(a)) and II (Fig. 4(b)) at frequency of radiation null 1.65 GHz, as well as Antennas II (Fig. 4(c)) and III (Fig. 4(d)) at 3.03 GHz. As shown in Fig. 4(a), very strong current distributes on the driven dipole of Antenna I, and rather weak current of anti-phase is observed on the director. Therefore, the radiation at this frequency is dominated by the driven dipole. When the reflector is introduced in Antenna II, it can be seen from Fig. 4(b) that the current distributions on the dipole and the director remain almost unchanged. However, considerable current is induced on the reflector, which is  $0^\circ$  in-phase with that on the director but  $180^\circ$  out-of-phase with the dipole. Consequently, the radiation of the dipole can be canceled out by the summational radiation caused by the director and the reflector, leading to a radiation null in the end-fire direction at 1.65 GHz. The current distributions at 3.03 GHz are found quite different, but the generative mechanism of the null is similar. With reference to Fig. 4(c) and Fig. 4(d), the current on the reflector becomes very weak and even negligible in

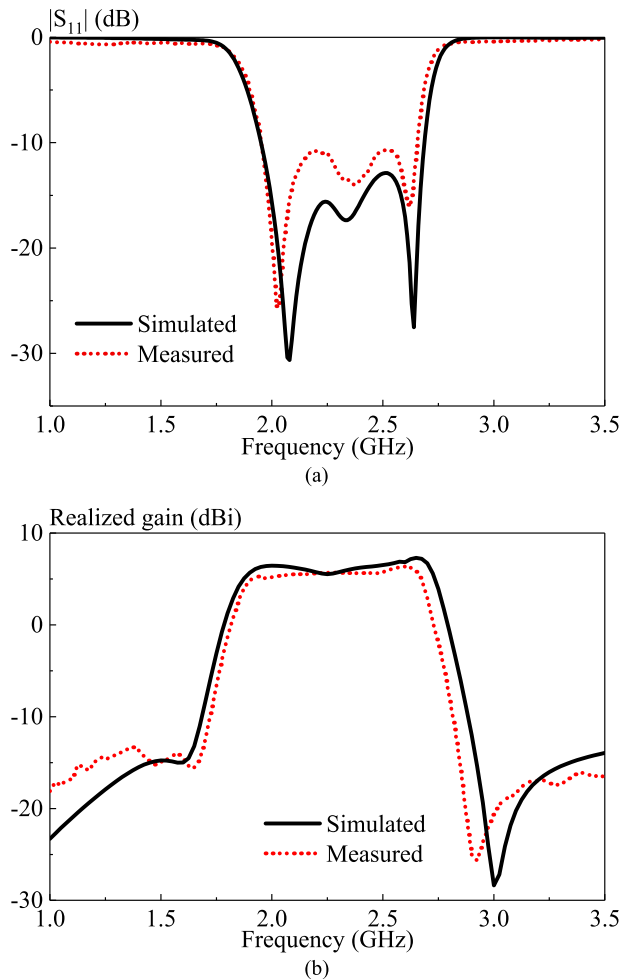


FIGURE 10. Simulated and measured reflection coefficients and end-fire gains of the prototype. (a) Reflection coefficients. (b) End-fire gains.

both Antennas II and III. Moreover, the currents are of anti-phase on the left and right sides. It means the effect of the reflector can be neglected at this frequency. In Antenna II, the current on the dipole is much stronger than that on the director, and therefore the radiation in the end-fire direction is considerable. However, in Antenna III, strong current is coupled to the parasitic element, balancing that on the director and the dipole. A radiation null at 3.03 GHz is therefore achieved owing to the cancellation effect.

The mechanisms of the two radiation nulls (1.58 and 3.01 GHz) in the proposed antenna are nearly the same, and therefore not discussed here repeatedly. Instead, the far-field radiation patterns of the proposed antenna and the reference Antenna I at the null frequencies are compared in Fig. 5, validating the above discussions.

#### D. PARAMETRIC STUDY

A parametric study has been carried out to further characterize the proposed filtering antenna. The simulated reflection coefficients, end-fire gains for different lengths of the reflector ( $l_2$ ) as well as the parasitic element ( $l_3$ ) are shown in Fig. 6 and Fig. 7, respectively. It can be observed from

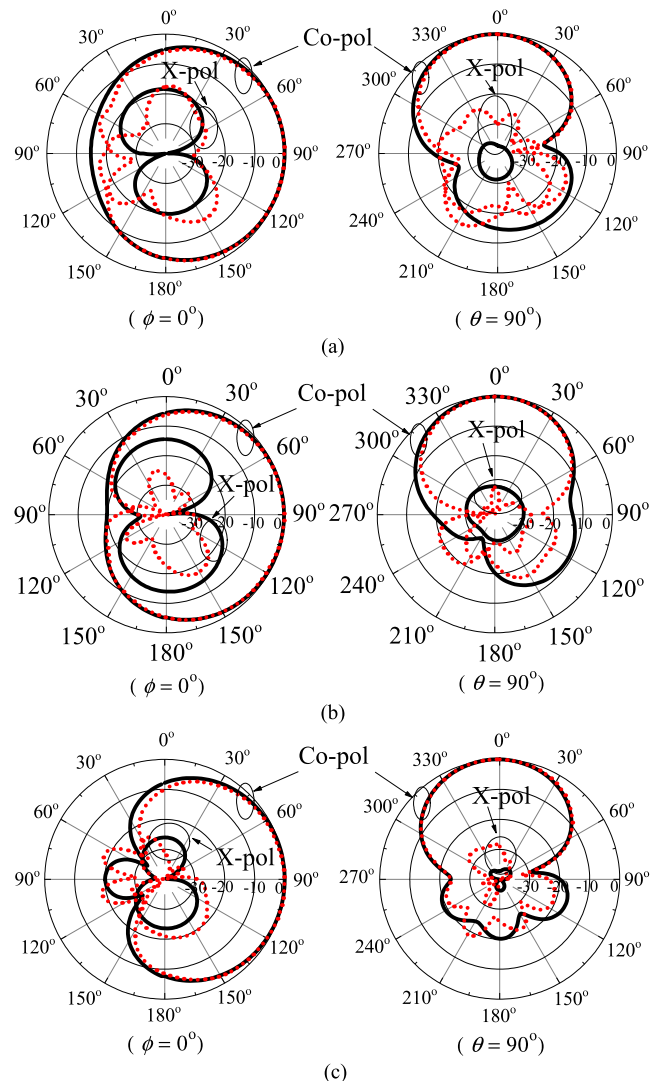


FIGURE 11. Simulated and measured radiation patterns of the prototype. (a) 2.08 GHz. (b) 2.34 GHz. (c) 2.64 GHz.

— Simulated ····· Measured.

Fig. 6 that as  $l_2$  decreases from 70 to 54 mm, the response in the upper band is nearly unaffected. However, the impedance matching in the lower band is significantly degraded, and moreover, the radiation null at the lower band-edge shifts upwards accordingly. On the contrary, it can be seen from Fig. 7 that the variation of  $l_3$  has little effect on the input impedance, radiation null and suppression level in the lower stopband. However, the third resonance and the radiation null at the upper band-edge move downwards with the increase of  $l_3$ . In addition, the effects of the spacing ( $s_3$ ) between the dipole and parasitic element have also been studied and shown in Fig. 8. With reference to the figure, the parameter  $s_3$  affects the impedance matching within the passband substantially, but hardly has any effect on the antenna gain and the filtering response.

In general, it can be concluded that the lower and upper filtering response can be independently adjusted by tuning the parasitic element and reflector respectively, whereas the



**TABLE 2.** Comparisons with the previous reported filtering quasi-Yagi antennas.

Ref	Frequency (GHz)	BW (%)	Gain (dBi)	Size ( $\lambda_0 \times \lambda_0$ )	Radiation null	Out-of band suppression (dB)	Extra filtering circuits	Feeding structure
[16]	2.5	48	4	$1.0 \times (>0.91)$	0	-	Yes	a balanced-to-unbalanced bandpass filter
[17]	1.72	16.7	5.5	$0.57 \times (>0.5)$	0	24	Yes	a multilayer balun filter
[18]	1.81	5.5	5.3	$0.6 \times (>0.54)$	0	18	Yes	a DSPSL filter
[19]	5.2	25	4.8	-	1	15	Yes	a multimode-resonator based filter
[20]	4.4	34.1	4.6	$0.81 \times 0.51$	5	9	Yes	a bandstop filter
[21]	3.04	56.6	4.9	$0.61 \times (>0.37)$	1	9	No	a coaxial cable coated with a bazoooka balun
This work	2.3	30.4	5.7	$0.54 \times 0.38$	2	19	No	a balanced DSPSL

$\lambda_0$ : the free-space wavelength at the center frequency.

impedance matching within the passband can be controlled by adjusting the spacing between the dipole and parasitic element without affecting the filtering response. These features greatly facilitate the design of the filtering antenna.

### III. MEASUREMENT RESULTS AND DISCUSSIONS

A prototype of the proposed quasi-Yagi antenna working at 2.4 GHz was fabricated and measured. Fig. 9 shows two photographs of the prototype, which was fabricated on a PCB of F4B with  $\epsilon_r = 2.94$  and  $h = 0.8$  mm. All the parameters are the same as in Table 1. A coaxial cable was used to feed the antenna, with its inner and outer conductors connecting to the two strip lines of the DSPSL. In this paper, the reflection coefficients were measured by a Keysight E5071C vector network analyzer, while the antenna gains and radiation patterns were obtained by a Satimo Starlab system.

Fig. 10(a) shows the measured and simulated reflection coefficients  $|S_{11}|$  of the prototype. A reasonable agreement is obtained between the simulation and measurement, and the small discrepancy is primarily due to the fabrication tolerance and experiment error. There are three resonant modes excited in the passband, at 2.03, 2.37 and 2.62 GHz, respectively. The measured  $-10$ -dB impedance bandwidth is given by 30.4%, ranging from 1.95 to 2.65 GHz. The reflection coefficient increases rapidly to near 0 dB at both band-edges and remains about 0 dB in the near stopbands, showing good filtering response.

The simulated and measured end-fire gains of the prototype are shown in Fig. 10(b). Again, a reasonable agreement is observed. The measured end-fire gain varies gradually from 5.04 to 6.36 dBi across the operating band (1.95-2.65 GHz), but decreases quickly and significantly at the band-edges. Two radiation nulls are measured at 1.65 and 2.93 GHz, very close to the predicted result (1.58 and 3.01 GHz) of simulation. The out-of band radiation is as low as less than  $-14$  dB, indicating the suppression level is of more than 19 dB in both the lower and upper stopbands. A quasi-elliptic band-pass filtering response is well exhibited.

Fig. 11 shows the measured and simulated radiation patterns of the prototype in the  $xz$ -plane ( $H$ -plane) and the  $xy$ -plane ( $E$ -plane) at 2.08, 2.34, and 2.64 GHz, respectively. End-fire radiation patterns are obtained in both planes, and the patterns are very stable over the entire passband. The maximum radiation is found in the  $+x$  direction, and the measured front to back (F/B) ratio is of more than 19 dB. The antenna also has a low cross-polarization level of  $-28$  dB in the direction of the maximum radiation. Similar with the conventional quasi-Yagi antenna, the beam-width in the  $H$ -plane is reasonably wider than that in the  $E$ -plane.

A comprehensive comparison between the proposed filtering quasi-Yagi antenna and the previously reported designs is summarized in Table 2. According to the table, both band-pass filtering and end-fire radiating responses were realized in [16]–[20], but extra filtering circuits/filters were utilized in their feeding networks, resulting in relatively larger footprints and lower antenna gains. A compact filtering quasi-Yagi antenna was realized in [21] with the aid of a parasitic loop. However, a moderate filtering performance was obtained and the out-of band suppression level could only reach 10 dB. Moreover, a coaxial bazoooka balun was required, increasing the complexity of the feeding network. The proposed antenna is based on the balanced DSPSL structure, and therefore can be easily connected to a  $50\text{-}\Omega$  coaxial cable. In addition, the filtering response is realized by skillfully designing the reflector and the parasitic element, without the need of any filtering circuit. Two radiation nulls are generated at the band-edges of the passband, improving the roll-off rate significantly. Therefore, compared with the previous designs, the proposed antenna has the advantages of simple structure, compact size, high gain, and enhanced frequency selectivity.

### IV. CONCLUSION

A low profile, planar, quasi-Yagi filtering antenna based on the DSPSL structure has been investigated in this paper. It has been shown that induced current can be coupled on the reflector and parasitic element, which can not only generate

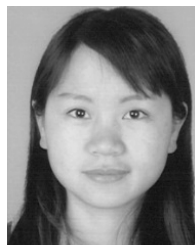
additional resonance to increase the bandwidth of operating passband, provide additional radiation to enhance the in-band antenna gain, but also can generate radiation nulls to suppress the out-of-band radiation. Both good bandpass filtering response and satisfying end-fire radiating characteristic can therefore be achieved without requiring any filtering circuit. A prototype working at 2.4 GHz has been fabricated and measured. The prototype has a  $-10$ -dB impedance bandwidth of 30.4%, a flat gain of about 5.7 dBi over the passband, and an out-of-band suppression level of about 20 dB in the stopbands.

## REFERENCES

- [1] C.-T. Chuang and S.-J. Chung, "Synthesis and design of a new printed filtering antenna," *IEEE Trans. Antennas Propag.*, vol. 59, no. 3, pp. 1036–1042, Mar. 2011.
- [2] C. X. Mao et al., "Dual-band patch antenna with filtering performance and harmonic suppression," *IEEE Trans. Antennas Propag.*, vol. 64, no. 9, pp. 4074–4077, Sep. 2016.
- [3] M.-C. Tang, Y. Chen, and R. W. Ziolkowski, "Experimentally validated, planar, wideband, electrically small, monopole filtennas based on capacitively loaded loop resonators," *IEEE Trans. Antennas Propag.*, vol. 64, no. 8, pp. 3353–3360, Aug. 2016.
- [4] J. Deng, S. Hou, L. Zhao, and L. Guo, "A reconfigurable filtering antenna with integrated bandpass filters for UWB/WLAN applications," *IEEE Trans. Antennas Propag.*, vol. 66, no. 1, pp. 401–404, Jan. 2018.
- [5] J.-F. Qian, F.-C. Chen, Y.-H. Ding, H.-T. Hu, and Q.-X. Chu, "A wide stopband filtering patch antenna and its application in MIMO system," *IEEE Trans. Antennas Propag.*, vol. 67, no. 1, pp. 654–658, Jan. 2019.
- [6] X. Y. Zhang, W. Duan, and Y.-M. Pan, "High-gain filtering patch antenna without extra circuit," *IEEE Trans. Antennas Propag.*, vol. 63, no. 12, pp. 5883–5888, Dec. 2015.
- [7] J. Y. Jin, S. Liao, and Q. Xue, "Design of filtering-radiating patch antennas with tunable radiation nulls for high selectivity," *IEEE Trans. Antennas Propag.*, vol. 66, no. 4, pp. 2125–2130, Apr. 2018.
- [8] Y. M. Pan, P. F. Hu, X. Y. Zhang, and S. Y. Zheng, "A low-profile high-gain and wideband filtering antenna with metasurface," *IEEE Trans. Antennas Propag.*, vol. 64, no. 5, pp. 2010–2016, May 2016.
- [9] P. F. Hu, Y. M. Pan, K. W. Leung, and X. Y. Zhang, "Wide-/dual-band omnidirectional filtering dielectric resonator antennas," *IEEE Trans. Antennas Propag.*, vol. 66, no. 5, pp. 2622–2627, May 2018.
- [10] Y. Li et al., "A nonbalancing end-fire microstrip dipole with periodic-offset DSPSL substrate," *IEEE Trans. Antennas Propag.*, vol. 65, no. 5, pp. 2661–2665, May 2017.
- [11] T.-G. Ma, C.-W. Wang, R.-C. Hua, and J.-W. Tsai, "A modified quasi-Yagi antenna with a new compact microstrip-to-coplanar strip transition using artificial transmission lines," *IEEE Trans. Antennas Propag.*, vol. 57, no. 8, pp. 2469–2474, Aug. 2009.
- [12] S. S. Jehangir and M. S. Sharawi, "A wideband sectoral quasi-Yagi MIMO antenna system with multibeam elements," *IEEE Trans. Antennas Propag.*, vol. 67, no. 3, pp. 1898–1903, Mar. 2019.
- [13] J. Shi, L. Zhu, N.-W. Liu, and W. Wu, "A microstrip Yagi antenna with an enlarged beam tilt angle via a slot-loaded patch reflector and pin-loaded patch directors," *IEEE Antennas Wireless Propag. Lett.*, vol. 18, no. 4, pp. 679–683, Apr. 2019.
- [14] N. Kaneda, W. R. Deal, Y. Qian, R. Waterhouse, and T. Itoh, "A broadband planar quasi-Yagi antenna," *IEEE Trans. Antennas Propag.*, vol. 50, no. 8, pp. 1158–1160, Aug. 2002.
- [15] L. Lu, K. Ma, F. Meng, and K. S. Yeo, "Design of a 60-GHz Quasi-Yagi antenna with novel ladder-like directors for gain and bandwidth enhancements," *IEEE Antennas Wireless Propag. Lett.*, vol. 15, pp. 682–685, 2016.
- [16] C.-H. Wu, C.-H. Wang, S.-Y. Chen, and C. H. Chen, "Balanced-to-unbalanced bandpass filters and the antenna application," *IEEE Trans. Microw. Theory Techn.*, vol. 56, no. 11, pp. 2474–2482, Nov. 2008.
- [17] H. Tang, J.-X. Chen, H. Chu, G.-Q. Zhang, Y.-J. Yang, and Z.-H. Bao, "Integration design of filtering antenna with load-insensitive multilayer balun filter," *IEEE Trans. Compon., Packag., Manuf. Technol.*, vol. 6, no. 9, pp. 1408–1416, Sep. 2016.
- [18] J. Shi et al., "A compact differential filtering quasi-Yagi antenna with high frequency selectivity and low cross-polarization levels," *IEEE Antennas Wireless Propag. Lett.*, vol. 14, pp. 1573–1576, 2015.
- [19] H.-W. Deng, T. Xu, and F. Liu, "Broadband pattern-reconfigurable filtering microstrip antenna with quasi-Yagi structure," *IEEE Antennas Wireless Propag. Lett.*, vol. 17, no. 7, pp. 1127–1131, Jul. 2018.
- [20] K.-D. Xu, H. Xu, and Y. Liu, "Low-profile filtering end-fire antenna integrated with compact bandstop filtering element for high selectivity," *IEEE Access*, vol. 7, pp. 8398–8403, Jan. 2019.
- [21] J. Wu, Z. Zhao, Z. Nie, and Q. H. Liu, "A printed unidirectional antenna with improved upper band-edge selectivity using a parasitic loop," *IEEE Trans. Antennas Propag.*, vol. 63, no. 4, pp. 1832–1837, Apr. 2015.
- [22] S.-G. Kim and K. Chang, "Ultrawide-band transitions and new microwave components using double-sided parallel-strip lines," *IEEE Trans. Microw. Theory Techn.*, vol. 52, no. 9, pp. 2148–2152, Sep. 2004.
- [23] W. Che, L. Gu, and Y. L. Chow, "Formula derivation and verification of characteristic impedance for offset double-sided parallel strip line (DSPSL)," *IEEE Microw. Wireless Compon. Lett.*, vol. 20, no. 6, pp. 304–306, Jun. 2010.
- [24] H. Xu, Y. Li, D. Ye, and Y. Long, "A broadband offset-parallel-parallelograms printed endfire antenna," *IEEE Antennas Wireless Propag. Lett.*, vol. 16, pp. 1167–1170, 2017.



**GUI LIU** was born in Guizhou, China. He received the B.Eng. degree in photoelectric information science and engineering from the South China University of Technology, Guangzhou, China, in 2018, where he is currently pursuing the M.Eng. degree with the School of Electronic and Information Engineering. His current research interests include filtering antennas and array antennas.



**YONG MEI PAN** was born in Huangshan, Anhui, China. She received the B.Sc. and Ph.D. degrees in electrical engineering from the University of Science and Technology of China, Hefei, China, in 2004 and 2009, respectively.

From 2009 to 2012, she was a Research Fellow with the Department of Electronic Engineering, City University of Hong Kong, Hong Kong. In 2013, she joined the School of Electronic and Information Engineering, South China University of Technology (SCUT), Guangzhou, China, as an Associate Professor. She is currently a Professor with SCUT. Her research interests include dielectric resonator antennas, leaky-wave antennas, metasurface antennas, and filtering antennas. She is currently an Associate Editor of the IEEE TRANSACTIONS ON ANTENNAS AND PROPAGATION.



**TIAN LI WU** was born in Changchun, Jilin, China. She received the B.Eng. degree in communication engineering from Southwest University, Chongqing, China, in 2015. She is currently pursuing the M.Eng. degree with the South China University of Technology, Guangzhou, China. Her research interests include filtering antennas and wide-band antennas.



**PENG FEI HU** (S'17) was born in Xiangyang, China. He received the B.Eng. degree in electronic and information engineering from Hainan University, Haikou, China, in 2014. He is currently pursuing the Ph.D. degree with the School of Electronic and Information Engineering, South China University of Technology, Guangzhou, China.

In 2016, he joined the Department of Electronic Engineering, City University of Hong Kong, Hong Kong, as a Research Assistant. His current research interests include filtering antennas, dielectric resonator antennas, and metasurface antennas.

...